MATCH
Communications in Mathematical and in Computer Chemistry

MATCH Commun. Math. Comput. Chem. **91** (2024) 307–336
ISSN: 0340–6253
doi: 10.46793/match.91-2.307M

Chaotic Behavior of Lorenz−Based Chemical System under the Influence of Fractals

Muhammad Marwan[a], Anda Xiong[b,*], Maoan Han[a], Ramla Khan[c]

[a] *School of Mathematical Sciences, Zhejiang Normal University, China.*
[b] *School of Systems Science, Institute of Non-Equilibrium Systems, Beijing Normal University, Beijing, China.*
[c] *School of Environment Earth and Ecosystem Sciences (EEES), The Open University, Milton Keynes MK76AA, UK*

marwan78642@zjnu.edu.cn [a], axiong23@wisc.edu [b], mahan@zjnu.edu.cn [a], ramla.khan@open.ac.uk [c]

(Received May 3, 2023)

Abstract

This research examines a chaotic chemical reaction system based on the variation of the Lorenz system. This study demonstrates that although the first phase portraits of the chemical models under consideration and the Lorenz models are comparable, they do not fully follow all the features of the Lorenz system. Questions about the existence of fractals in systems based on chemical reactions are addressed in the current work. Moreover, we have worked on the hidden information inside in each wings of a chaotic system generated through fractal process, for the first time, with the aid of basin for fractals. Additionally, we looked closely at the dynamics of the model across the basin, which revealed additional details regarding the existence of hidden and cyclic attractors inside each wing. We also produced multi-wings for system (1) in the current study, demonstrating in a general manner that the number of cyclic attractors increase in a direct relation to the number of wings. Moreover, Julia approach is used to accomplish the work of multi-wings,

*Corresponding author.

whereas for searching cyclic attractors inside each extra wing, we have used fifteen million initial conditions and compiled them as a basin set. The data generated in this work is also provided within this paper for the ease of readers.

1 Introduction

Everything in the universe is subject to change over time, and such variations are referred to as dynamics. In mathematics, the same concept exists with the emergence of field: nonlinear dynamics. Since the discovery of chaos in 1963, when Edwards Lorenz was working on weather model simulations, this discipline has received considerable attention. Eventually, such behavior came to be known as chaos and was defined as "the exponential sensitivity to initial conditions, dense orbits, and parameter values." Lorenz's publication directed researchers in a new direction. Since then, an enormous number of three-dimensional chaotic systems have been derived, such as Bouali [4], Sprott [35], Yu-Wang [50], and many others. This model was also presented in a variety of other physical-term-inclusive variants, and all of them are grouped together as the family of Lorenz-like systems [43]. However, Chen [5] generated the initial chaotic system with the aid of the Lorenz system; but their properties were distinct. The significance of chaotic systems extends beyond mathematics and has a variety of implications in other disciplines. Marwan et al. [27] applied the technique of observers with incremental quadratic constraints for fractional-ordered chaotic systems in 2022 as a method for the secure transmission of an image file. Guo et al. [9] designed an algorithm with variable parameters for chaotic systems in 2021 and implemented it in RFID-based security. Towards the end of 2019; a pandemic disease broke out, that quickly spread around the globe. This topic attracted researchers in various disciplines including the field of dynamics, who introduced several chaotic systems. Mangiarotti *et al.* applied chaos theory to the covid outbreak [24] and obtained superior results, whereas Jones [16] confirmed the existence of chaos in the Covid epidemic's spread. Similarly, the work of Iqbal *et al.* [12, 13] verifies the existence of chaos and controllability in Cancer systems, revealing additional applications of chaos in biological systems. Apart from the field of biological sciences, the term chaos has a variety of contribution in the applications of robotics [25, 31] and engineering [26, 37] as well.

Chemistry is one of the disciplines that contributes to the production of variety of beneficial real-world products,but a seemingly insignificant error during the performance of a chemical reaction can sometimes cause chaos. Multiple dynamical systems are founded on chemical reactions, but Rossler is the pioneer who introduced the first chaotic system based on biochemistry. Since then, numerous research papers on the Rossler system have been discovered, including [14,18,19,28] and their references. To comprehend chemical reactions in depth, mathematics is required as a prerequisite and for more information, combining chemistry with dynamical systems is one of the most significant combinations.

Ameen [1] recently examined a biochemical reaction system to discuss its numerous algebraic surfaces, exponential factors, and lack of integration. In recent research on oscillatory solutions and chaos, a chemical reaction involving two species [6] has been considered. In 2022, Din [7] examined a three-dimensional chaotic system without using its eigenvalues to determine the existence of Hopf bifurcation. Besides that, his investigation incorporates the property associated with the investigation of "bounds" using Lyapunov theory. Ibrahim and Peter used Chemical Organization Theory (OCT) to organize and identify the persistent subspaces of a system of ordinary differential equations [15]. Likewise, if every positive equilibrium is itself complex balanced, then such chemical systems are deemed Absolutely Complex Balanced (**ACB**). In 2022, Jose *et al.* [17] examined the same technique and concentrated on a few other kinetic systems. Furthermore, they have developed a novel method for **ACB** in kinetic systems. Ndlovu *et al.* [32] studied the hydrolysis of glycerol over a metal catalyst in 2022, resulting in a system of ordinary differential equations. They evaluated this system to investigate its qualitative behavior. Several other work on oscillatory solutions and their controllability in (integer and fractional) ordered dynamical systems are discussed in [20,33,45] and references therein.

Fractals are structures that repeats itself through a range of scaling, so that one observe similar pattern in different scales. Since such behavior is a consequence of the scaling-invariance of the forming mechanism, fractals are commonly observed in nature. In other terms, the more one moves inside, the more identical structures materialize. If fractals occur in chemical reactions, it means that the bonds between atoms break apart and then reform into small and similar structures. This concept demonstrates that fractals are an integral component of chemical reactions. In nature, fractals can be found in clouds, mountain ranges, ocean surges, earth strata, and much more. Beroit Mandel [29] introduced the function of complex numbers in fractals analysis. With the discovery of fractals, several nature-based concerns were resolved, and the universe's boundaries were disclosed to be without end [21, 38].

It is commonly observed that chaotic systems exhibit orbits of fractal structure, while a fractal structure does not necessarily leads to chaos. Nevertheless, if the fractal property is applied to chaotic systems, it may result in the formation of multiple identical wings. There are numerous techniques in the literature for generating analogous wings in chaotic systems, but Miranda and Stone [30], who proposed a proto-Lorenz system, are credited with initiating this topic. This prototype system was based on the original system's additional wings, but their study was limited to six wings only. Following their work, Guo *et al* [10] provided the generalized analytical formulae for the generation of multi-wings in chaotic systems. In 2017, Azam *et al* [2] used the same formulae and proved the existence of multi-wings into STF chaotic model. In addition, there are further several more effective methodologies used to generate multi-wings in chaotic systems including switching manifolds [44], step function [51], jerk circuits [52] and much more [11, 22, 23, 39, 40, 53]. But recently Azam *et al* [3] designed an algorithm for the existence of generalized multi-wings in all directions for chaotic system.

Basins, a well-known concept in the field of nonlinear sciences have a similar structure to fractals except basins are sets of initial points in phase space. In addition, if the initial points in a phase lead to an attracting set, such sets are known as basins of attractors. Basins have a wide range of applications in terms of discovering chaos, limit cycles, bifurcations, and much more, but their interesting structures can also result in the existence of similar shapes. The most recent study of the basin was conducted by Datseris [8], who presented an automated technique for identifying attractors without taking its dynamics into account. Similarly, Sprott and Xiong [41] classified basins of attraction in a variety of scenario and later investigated basins of tri-stability [46] for the first time in the Lorenz system to gain more insight and detail. In 2022, Marwan *et al.* [26] utilized the same method for locating basins in a mechanical-based system and discussed its basin in two and three dimensions.

The aforementioned citation regarding chemical models demonstrates that these systems are of great interest but are primarily discussed using two-dimensional models. However, there are two chemical models based on (Lorenz [34] and Chua [47]) chaotic systems in which Xu *et al.* [48, 49] performed work on chemical chaotic systems based on the Chua system from multiple perspectives, but the chemical chaotic model based on the Lorenz system has been ignored for the past three decades. Therefore, in this paper, we examine the Lorenz−based chemical model [34], which spawned the following queries after reviewing the aforementioned works and surveying the relevant literature.

1. If there exists chaos in systems based on chemical reactions then why not fractals?

2. If fractals in chaotic systems generate similar chaotic wings, then what about the basins of fractal?

3. What is hidden inside in each wing of a chaotic system generated through fractal process?

4. Is the basin always leading to attracting set?

We found that the above questions remain unanswered in the literature of chemistry and dynamical systems. Keeping in mind the above questions, we studied the dynamics of a Lorenz−based chaotic system including chemical processes whose initial phase portrait resembles that of the Lorenz system, but other properties are distinct. Furthermore, we used the Julia concept to generate multi-wings in a chemical-reaction system and classified basins for fractals of the system under consideration. While investigating the basins of system (1), we discovered that there exist cyclic attractors that have a direct correlation with the number of generated wings. Researchers in various fields of nonlinear systems now have a new avenue to explore because of the discovery of cyclic attractors embedded inside each wing.

This paper is structured in the following manner: In section (2), a chemical reaction model is considered, its initial conditions and parameter values are also given there to show the existence of chaos, whereas its physical properties and chemical reactions that made a foundation for the modelling of our considered system (1) are explained in Appendix **A**. Several dynamical properties of system (1) including equilibrium points, symmetrical rotation, volume dissipation and existence of various other attractors are discussed in section (3). The process of fractals for the generation of four and six wings of our considered system are proved analytically and shown numerically in section (4). This section also includes the study of basins of fractals and the existence of cyclic attractors in each wing. In section (5), a random high wing is created using the analytical formulae given in Appendix **B**, while section (6) consist of concluding remarks about our paper.

2 Chemical reaction Lorenz–based system

The model considered in this paper is the modification of Lorenz system and is taken from the work of Poland [34]:

$$\begin{cases} \dot{\mathfrak{p}_1} = -k_1\mathfrak{p}_1 + k_2\mathfrak{p}_2 \\ \dot{\mathfrak{p}_2} = k_3\mathfrak{p}_1 - k_4\mathfrak{p}_2 + k_5\mathfrak{p}_3 - k_6\mathfrak{p}_1\mathfrak{p}_3 + k_7 \\ \dot{\mathfrak{p}_3} = -k_8\mathfrak{p}_1 - k_9\mathfrak{p}_2 - k_{10}\mathfrak{p}_3 + k_{11}\mathfrak{p}_1\mathfrak{p}_2 + k_{12}, \end{cases} \tag{1}$$

where k_i for $i = 1, 2, \cdots, 12$ are constant rates (parameters) of system (1) and $\mathfrak{p}_1$, $\mathfrak{p}_2$, $\mathfrak{p}_3$ shows the concentration of X, Y, Z, where X is catalysed by and the out flux from Y is catalysed by Z. System (1) is chaotic for initial conditions ($\mathfrak{p}_1$, $\mathfrak{p}_2$, $\mathfrak{p}_3$)=(0.01, 0.01, 23.3) and parameter values given in Table (1). However, the model is same, but we have selected different

Table 1. Symbolic and numerical values of parameters involved in system (1)

Parameter	Symbolic Value	Numerical Value
$k_1 = k_2$	ζ	10
$k_4=k_6=k_{11}$	1	1
$k_5=k_8=k_9$	μ	14
k_3	$(\varrho + \mu)$	38.4000
k_7	$(\mu - \varrho\mu - \mu^2)$	-523.6000
k_{10}	α	28
k_{12}	$(\mu^2 + \alpha\mu)$	233.3333

parameter values along with initial conditions for the existence of chaos, where μ is the axis shifted value, used for the transformation of Lorenz into chemical reactions-based system. The existence of nonlinear terms in dynamical systems are rare but in chemical reactions-based models it was a big trouble. For-example the appearance of $\mathfrak{p}_1\mathfrak{p}_3$ in $\dot{\mathfrak{p}_2}$ was a question that why it does not appear in $\dot{\mathfrak{p}_1}$ and $\dot{\mathfrak{p}_3}$. Therefore, the transformation method was introduced in such type of systems to solve the issue but was not that effective. Then, in 1983, Toth and Hars [42] found a way by considering $\mathfrak{p}_1$ and $\mathfrak{p}_3$ terms as a catalyst whose concentration does not bring changes in the chemical reaction. Similar is the case for other nonlinear terms as well. Moreover, further explanation about the model (1) is given in Appendix **A**.

3 Dynamical properties

Fig. 1 is the phase portrait of system (1) and looks like original Lorenz system but still exhibits different properties.

3.1 Equilibrium points

Equilibrium points are the first step for building blocks of various aspects in any dynamical systems. Our considered model has the following three

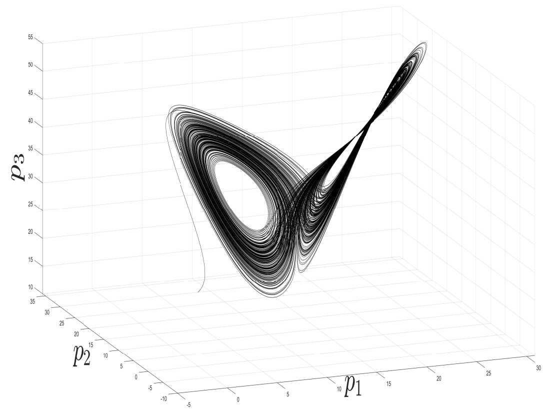

Figure 1. Chaotic trajectories in system (1)

equilibrium points:

$$\begin{cases} \varepsilon_\mu = (\mu, \mu, \mu) \\ \varepsilon_2 = (\mu - \sqrt{\alpha\varphi}, \mu - \sqrt{\alpha\varphi}, \mu + \varphi) \\ \varepsilon_2 = (\mu + \sqrt{\alpha\varphi}, \mu + \sqrt{\alpha\varphi}, \mu + \varphi) \end{cases} \tag{2}$$

where $\varphi{=}(\varrho{-}1)$. One can get equilibrium points of original Lorenz system by setting μ equals to zero into Eq. (2).

Remark. For μ, α, $\varrho \in \mathbb{R}^+$ there exist three equilibrium points (2), while for $\alpha < 0$ or $\varrho < 1$ there exists single equilibrium point; ε_μ.

3.2 Volume dissipation & non-symmetrical rotation

Here we discuss the contraction of system (1). The Lorenz−based chemical system (1) has two non-linearities but the system has no rotational symmetry. One can also observe this property from the equilibrium points (2), where the addition of extra term μ has diminished the symmetrical property about any axis. Mathematically one can show this property by replacing the state variables $(\mathfrak{p}_1, \mathfrak{p}_2, \mathfrak{p}_3)$ with $(-\mathfrak{p}_1, \mathfrak{p}_2, -\mathfrak{p}_3)$, $(-\mathfrak{p}_1, -\mathfrak{p}_2, \mathfrak{p}_3)$, $(\mathfrak{p}_1, -\mathfrak{p}_2, -\mathfrak{p}_3)$ or $(-\mathfrak{p}_1, -\mathfrak{p}_2, -\mathfrak{p}_3)$ but in all cases the transformed systems do not approaches to original state variables. However, our considered model obeys the dissipation of volume by computing the gradient of system (1):

$$\nabla h = \sum_{L=\mathfrak{p}_1,\mathfrak{p}_2,\mathfrak{p}_3} \frac{\partial \dot{L}}{\partial L} = -(\zeta + \alpha + 1). \tag{3}$$

Using divergence theorem, $\dot{E} = -(\zeta + \alpha + 1)E$, where E shows the volume in phase space. The volume decreases exponentially by solving $\dot{E}$ and clearly this shows that system (1) is dissipative.

3.3 Existence of various types of attractors

The basin is the set of initial states in the phase space that heads towards the attracting set. Hence, if the initial points in a set are attracting towards an attractor, then the basin is famous for basin of attraction. Equivalently as the infinity behaves like an attracting set. This type of incident opens a new type of attractors. In this section, we have considered system (1) for the searching of several other types of attractors. Therefore, we have used ten million data set of initial points (which are also provided with the paper) for Fig. 2 that leads to the exploration of several regions. In Fig.

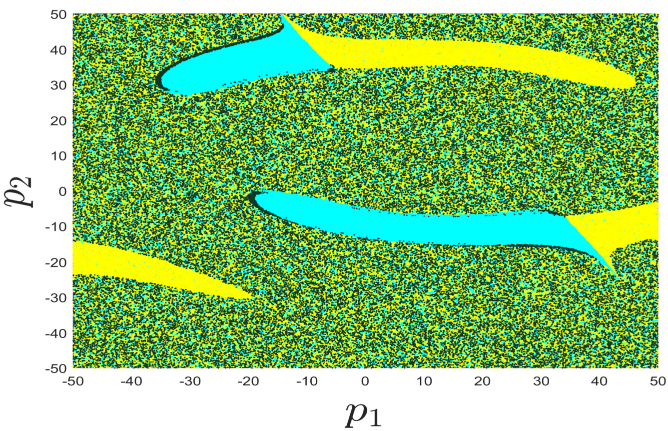

Figure 2. Basin of attraction of system (1) elaborating various type of attractors

2, one can see initial conditions, with Green and Yellow colours, help in the creation of yellow, blue and green sets. Each set shows distinct types of attractors. Therefore, to explain Fig. 2 in more depth, we give names to each set:

1. A_1:={Set of all initial points, where yellow and green points are intermingled with each other.}

2. A_2:={Set of all initial points, where only green points exist.}

3. A_3:={Set of all initial points, where only yellow points exist.}

4. A_4:={Set of all initial points, where there exist neither green nor yellow points.}

Moreover, we have selected initial points from each set to plot and explore what each set represents. In Figs. 3 and 4, we have selected initial points

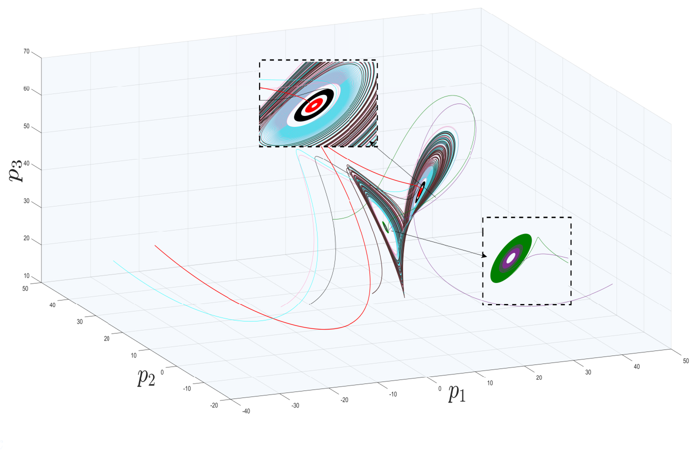

Figure 3. Cyclic, Hidden and Original attractors in system (1).

from each set to visualize the data sets of each domain. Fig. 3 is the $3D$ phase portrait, where different coloured trajectories are shown, while Fig. 4 is the same figure in different planes. First, we started selecting random points from set A_1 and get that each point in this set represents *chaotic attractor*. Then, we moved from set A_1 to A_2, which is further divided into

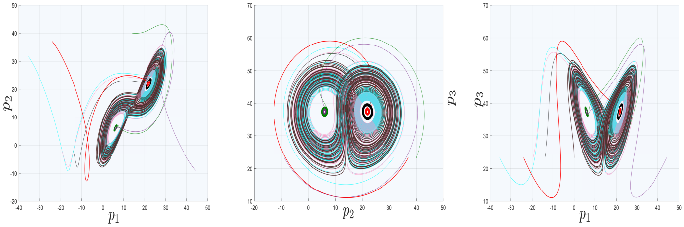

(a) $\mathfrak{p}_1 - \mathfrak{p}_2$ (b) $\mathfrak{p}_2 - \mathfrak{p}_3$ (c) $\mathfrak{p}_1 - \mathfrak{p}_3$

Figure 4. Two-dimensional phase portraits of Fig. 2 in various planes

two sub-regions (Above and Below). Moreover, we have selected light (blue and orange) colours for achieving the phase portraits of set A_2. In both Figs. 3 and 4, one can see that these trajectories are also chaotic, and one can say that points in set A_2 are leading towards *Hidden attractor*. After that, moving to set A_3, where we have observed that these set of initial conditions are heading towards the creation of *cyclic attractors* inside the empty space in left wing of original system (1), while the points in set A_4 also shows the existence of *cyclic attractors* in right wing of system (1). The more interesting result was the covering property of hidden attractor, where the points in set A_2 also work as a cover for the points in set A_4. This concept can also be seen in Fig. 2, where a cover occupies the outer edges of the white region.

4 Four and six wings fractals in system (1)

There exist many techniques in literature for the creation of fractals in dynamical systems [3,11,22,23,39,40,44,51–53], in which Julia [2] is one of the important techniques. This method is applied to system (1) to produce a chaotic system based on four and six wings. In this section, we have proved two theorems for the creation of extra wings in the Lorenz−based chemical system (1). Moreover, system (1) can be rewritten in terms of

$(\mathfrak{u}, \mathfrak{v}, \mathfrak{w})$ as;

$$\begin{cases} \dot{\mathfrak{u}} = -k_1\mathfrak{u} + k_2\mathfrak{v} \\ \dot{\mathfrak{v}} = k_3\mathfrak{u} - k_4\mathfrak{v} + k_5\mathfrak{w} - k_6\mathfrak{u}\mathfrak{w} + k_7 \\ \dot{\mathfrak{w}} = -k_8\mathfrak{u} - k_9\mathfrak{v} - k_{10}\mathfrak{w} + k_{11}\mathfrak{u}\mathfrak{v} + k_{12}. \end{cases} \tag{4}$$

The following two theorems play vital role in the generation of multi-wings chaotic attractors.

Theorem 1. *Let us define a surjective mapping* $\pi_1 : A(X) \to B(U)$ *as;*

$$\mathfrak{u} = \mathfrak{p}_1^2 - \mathfrak{p}_2^2, \ \ \mathfrak{v} = 2\mathfrak{p}_1\mathfrak{p}_2, \ \ \mathfrak{w} = \mathfrak{p}_3 \tag{5}$$

then system (1) *exhibit four wings and two similar attractors using transformation* $U = \wp_1 X$*, where* $U = (\mathfrak{u}, \mathfrak{v}, \mathfrak{w})$ *and* $X = (\mathfrak{p}_1, \mathfrak{p}_2, \mathfrak{p}_3)$*.*

Proof. We begin proof of Theorem 1 with the Jacobian matrix of transformation (5):

$$\wp_1 = \begin{pmatrix} 2\mathfrak{p}_1 & -2\mathfrak{p}_2 & 0 \\ 2\mathfrak{p}_2 & 2\mathfrak{p}_1 & 0 \\ 0 & 0 & 1 \end{pmatrix}. \tag{6}$$

Differentiating the inverse of transformation $X = \wp_1^{-1}U$, with $\wp_1^{-1}$ as inverse of the Jacobian matrix (6)

$$\begin{pmatrix} \dot{\mathfrak{p}}_1 \\ \dot{\mathfrak{p}}_2 \\ \dot{\mathfrak{p}}_3 \end{pmatrix} = \begin{pmatrix} \frac{\mathfrak{p}_1}{2\left(\mathfrak{p}_1^2+\mathfrak{p}_2^2\right)} & \frac{\mathfrak{p}_2}{2\left(\mathfrak{p}_1^2+\mathfrak{p}_2^2\right)} & 0 \\ -\frac{\mathfrak{p}_2}{2\left(\mathfrak{p}_1^2+\mathfrak{p}_2^2\right)} & \frac{\mathfrak{p}_1}{2\left(\mathfrak{p}_1^2+\mathfrak{p}_2^2\right)} & 0 \\ 0 & 0 & 1 \end{pmatrix} \begin{pmatrix} \dot{\mathfrak{u}} \\ \dot{\mathfrak{v}} \\ \dot{\mathfrak{w}} \end{pmatrix}. \tag{7}$$

To expand the velocity terms $(\dot{\mathfrak{u}}, \dot{\mathfrak{v}}, \dot{\mathfrak{w}})$ in Eq. (7), we use Eq. (5) to replace back $(\mathfrak{u}, \mathfrak{v}, \mathfrak{w})$ with $(\mathfrak{p}_1, \mathfrak{p}_2, \mathfrak{p}_3)$ to get system of the form:

$$
\begin{aligned}
\dot{\mathfrak{p}_1} =& \frac{\mathfrak{p}_1}{2\left(\mathfrak{p}_1^2+\mathfrak{p}_2^2\right)}\left[-k_1\left(\mathfrak{p}_1^2-\mathfrak{p}_2^2\right)+k_2\left(2\mathfrak{p}_1\mathfrak{p}_2\right)\right] \\
&+\frac{\mathfrak{p}_2}{2\left(\mathfrak{p}_1^2+\mathfrak{p}_2^2\right)}\left[k_3\left(\mathfrak{p}_1^2-\mathfrak{p}_2^2\right)-k_4\left(2\mathfrak{p}_1\mathfrak{p}_2\right)+k_5\mathfrak{p}_3-k_6\left(\mathfrak{p}_1^2-\mathfrak{p}_2^2\right)\mathfrak{p}_3+k_7\right], \\
\dot{\mathfrak{p}_2} =& \frac{\mathfrak{p}_1}{2\left(\mathfrak{p}_1^2+\mathfrak{p}_2^2\right)}\left[k_3\left(\mathfrak{p}_1^2-\mathfrak{p}_2^2\right)-k_4\left(2\mathfrak{p}_1\mathfrak{p}_2\right)+k_5\mathfrak{p}_3-k_6\left(\mathfrak{p}_1^2-\mathfrak{p}_2^2\right)\mathfrak{p}_3+k_7\right] \\
&-\frac{\mathfrak{p}_2}{2\left(\mathfrak{p}_1^2+\mathfrak{p}_2^2\right)}\left[-k_1\left(\mathfrak{p}_1^2-\mathfrak{p}_2^2\right)+k_2\left(2\mathfrak{p}_1\mathfrak{p}_2\right)\right], \\
\dot{\mathfrak{p}_3} =& -k_8\left(\mathfrak{p}_1^2-\mathfrak{p}_2^2\right)-k_9\left(2\mathfrak{p}_1\mathfrak{p}_2\right)-k_{10}\mathfrak{p}_3+k_{11}\left(\mathfrak{p}_1^2-\mathfrak{p}_2^2\right)\left(2\mathfrak{p}_1\mathfrak{p}_2\right)+k_{12}.
\end{aligned}
\tag{8}
$$

Equation (8) is our desired system, which creates four wings (two similar attractors) of our considered model (1). ■

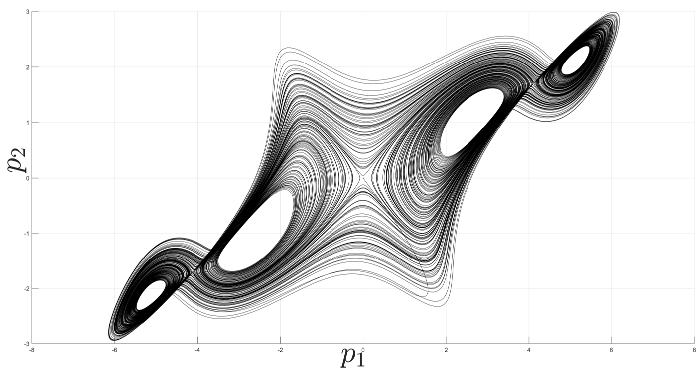

Figure 5. System (1) with four wings.

In Fig. 5, we can see the two similar chaotic attractors with four wings. This figure is generated using Eq. (8) with initial conditions and parameter values same as original system (1). However, its basin of attraction is part of the most interest. Similar to the basin of attraction (can be seen in Fig. 2) for original system, we have plotted the set of all initial points of system (8) to discuss the existence of various attractors. Fig. 6 presents the discussed basins, where three regions can be seen. Similarly, we categorized each set as:

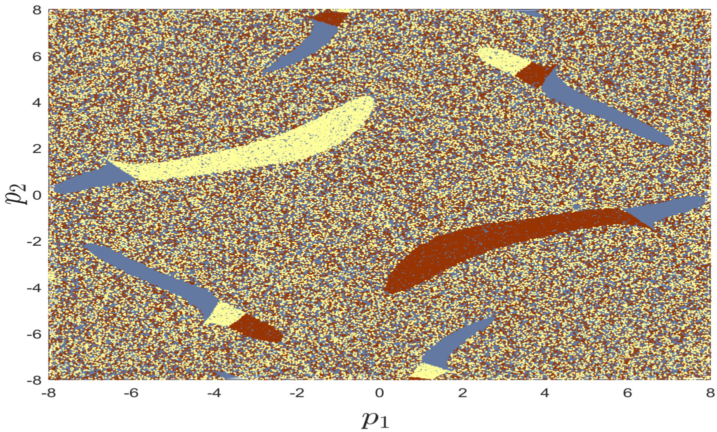

Figure 6. Basin of attraction of fractals-based system (8)

1. B_1:={Set of initial points, covered with yellow colour.}
2. B_2:={Set of initial points, covered with Brown colour.}
3. B_3:={Set of initial points, covered with Grey colour.}

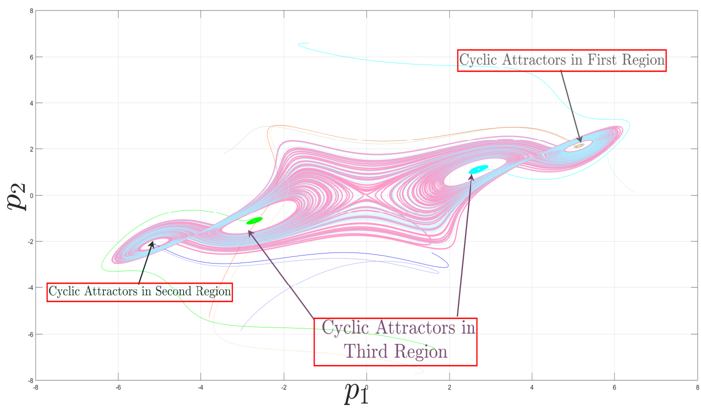

Figure 7. Existence of Cyclic attractors in each wing of system (8) and a Hidden attractor.

Fig. 7 is the visual validation of figure 6, where some points are considered from each set and plotted accordingly. Here, one can see four cyclic attractors and single Hidden attractor. For getting this figure, we have started selection of initial points from set B_1 and got cyclic attractors in right far wing of system (8). In similar fashion, initial points belong to set B_2 converges to attractor in left far wing, whereas the two grey coloured regions are categorized as: grey coloured initial points in set B_3 near to set B_1 converges to right wing near to centre, whereas points near to set B_2 started converging left wing near to centre.

Theorem 2. *Let us define a surjective mapping* $\pi_2 : A(X) \to B(U)$ *as;*

$$\mathfrak{u} = {\mathfrak{p}_1}^3 - 3\,\mathfrak{p}_1\,{\mathfrak{p}_2}^2, \;\; \mathfrak{v} = 3\,{\mathfrak{p}_1}^2\,\mathfrak{p}_2 - {\mathfrak{p}_2}^3, \;\; \mathfrak{w} = \mathfrak{p}_3 \tag{9}$$

then system (1) *exhibit four wings and two similar attractors using transformation* $U = \wp_1 X$*, where* $U = (\mathfrak{u}, \mathfrak{v}, \mathfrak{w})$ *and* $X = (\mathfrak{p}_1, \mathfrak{p}_2, \mathfrak{p}_3)$.

Proof. We begin proof of Theorem 2 with the Jacobian matrix of transformation (9):

$$\wp_1 = \begin{pmatrix} 3\mathfrak{p}_1^2 - 3\mathfrak{p}_2^2 & -6\mathfrak{p}_1\mathfrak{p}_2 & 0 \\ -6\mathfrak{p}_1\mathfrak{p}_2 & 3\mathfrak{p}_1^2 - 3\mathfrak{p}_2^2 & 0 \\ 0 & 0 & 1 \end{pmatrix}. \tag{10}$$

Differentiating the inverse of transformation $X = \wp_2^{-1}U$, with $\wp_2^{-1}$ as inverse of the Jacobian matrix (10)

$$\begin{pmatrix} \dot{\mathfrak{p}_1} \\ \dot{\mathfrak{p}_2} \\ \dot{\mathfrak{p}_3} \end{pmatrix} = \begin{pmatrix} \Omega_1 & \Omega_2 & 0 \\ -\Omega_2 & \Omega_1 & 0 \\ 0 & 0 & 1 \end{pmatrix} \begin{pmatrix} \dot{\mathfrak{u}} \\ \dot{\mathfrak{v}} \\ \dot{\mathfrak{w}} \end{pmatrix}, \tag{11}$$

where

$$\begin{cases} \Omega_1 = \frac{{\mathfrak{p}_1}^2 - {\mathfrak{p}_2}^2}{3\,({\mathfrak{p}_1}^2 + {\mathfrak{p}_2}^2)^2} \\ \Omega_2 = \frac{2\,\mathfrak{p}_1\,\mathfrak{p}_2}{3\,({\mathfrak{p}_1}^2 + {\mathfrak{p}_2}^2)^2}. \end{cases} \tag{12}$$

To expand the velocity terms $(\dot{\mathfrak{u}}, \dot{\mathfrak{v}}, \dot{\mathfrak{w}})$ in Eq. (11), we use Eq. (9) to replace back $(\mathfrak{u}, \mathfrak{v}, \mathfrak{w})$ with $(\mathfrak{p}_1, \mathfrak{p}_2, \mathfrak{p}_3)$ to get system of the form:

$$
\begin{aligned}
\dot{\mathfrak{p}_1} =& \frac{{\mathfrak{p}_1}^2 - {\mathfrak{p}_2}^2}{3\left({\mathfrak{p}_1}^2 + {\mathfrak{p}_2}^2\right)^2} \left[-k_1\left(\mathfrak{p}_1^3 - 3\,\mathfrak{p}_1\,\mathfrak{p}_2^2\right) + k_2\left(3\,\mathfrak{p}_1^2\,\mathfrak{p}_2 - \mathfrak{p}_2^3\right)\right] \\
&+ \frac{2\,\mathfrak{p}_1\,\mathfrak{p}_2}{3\left({\mathfrak{p}_1}^2 + {\mathfrak{p}_2}^2\right)^2} \left[k_3\left(\mathfrak{p}_1^3 - 3\,\mathfrak{p}_1\,\mathfrak{p}_2^2\right) - k_4\left(3\,\mathfrak{p}_1^2\,\mathfrak{p}_2 - \mathfrak{p}_2^3\right) + k_5\mathfrak{p}_3\right. \\
&\left.-k_6\left(\mathfrak{p}_1^3 - 3\,\mathfrak{p}_1\,\mathfrak{p}_2^2\right)\mathfrak{p}_3 + k_7\right], \\
\dot{\mathfrak{p}_2} =& \frac{2\,\mathfrak{p}_1\,\mathfrak{p}_2}{3\left({\mathfrak{p}_1}^2 + {\mathfrak{p}_2}^2\right)^2} \left[k_3\left(\mathfrak{p}_1^3 - 3\,\mathfrak{p}_1\,\mathfrak{p}_2^2\right) - k_4\left(3\,\mathfrak{p}_1^2\,\mathfrak{p}_2 - \mathfrak{p}_2^3\right) + k_5\mathfrak{p}_3\right. \\
&\left.-k_6\left(\mathfrak{p}_1^3 - 3\,\mathfrak{p}_1\,\mathfrak{p}_2^2\right)\mathfrak{p}_3 + k_7\right] - \frac{{\mathfrak{p}_1}^2 - {\mathfrak{p}_2}^2}{3\left({\mathfrak{p}_1}^2 + {\mathfrak{p}_2}^2\right)^2} \times \\
&\left[-k_1\left(\mathfrak{p}_1^3 - 3\,\mathfrak{p}_1\,\mathfrak{p}_2^2\right) + k_2\left(3\,\mathfrak{p}_1^2\,\mathfrak{p}_2 - \mathfrak{p}_2^3\right)\right], \\
\dot{\mathfrak{p}_3} =& -k_8\left(\mathfrak{p}_1^3 - 3\,\mathfrak{p}_1\,\mathfrak{p}_2^2\right) - k_9\left(3\,\mathfrak{p}_1^2\,\mathfrak{p}_2 - \mathfrak{p}_2^3\right) - k_{10}\mathfrak{p}_3 + k_{11}\mathfrak{u}\mathfrak{v} + k_{12}.
\end{aligned}
\tag{13}
$$

Equation (13) is our desired system, which generate six wings (three similar attractors) of our considered model (1). ■

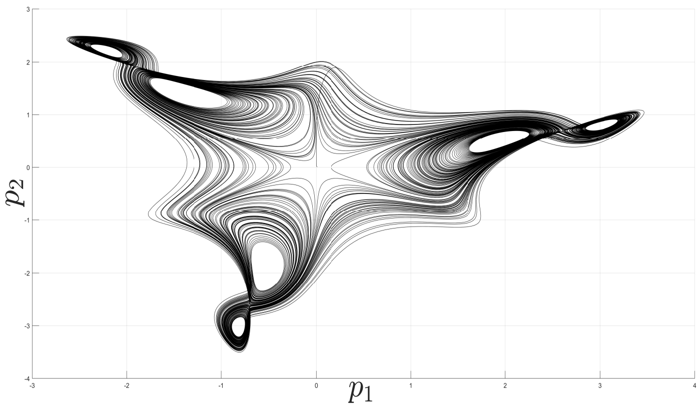

Figure 8. Six wings of system (1) using Eq. (13)

In Fig. 8, one can observe three similar chaotic attractors with six wings. This figure is generated using Eq. (13) with initial conditions and parameter values same as original system (1). The more we are increasing numbers of wings in our considered model, the more fascinating and

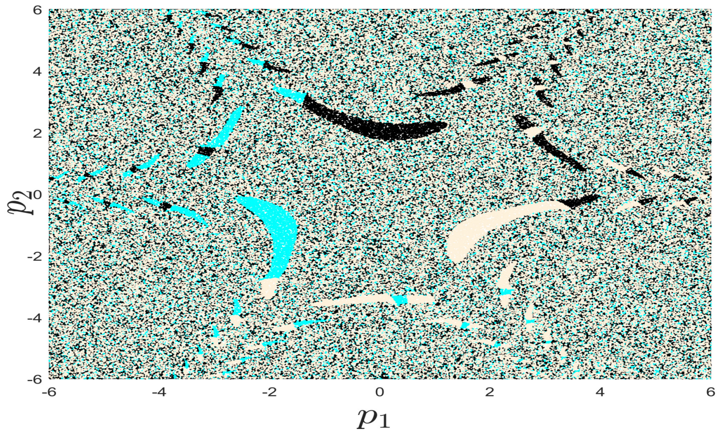

Figure 9. Basin of attraction of system (13) having six wings.

complex basins we are getting. Fig. 9 shows the required basin for system (13), which is categorized in three coloured regions as

1. C_1:={Set of initial points, covered with Black colour.}
2. C_2:={Set of initial points, covered with Cyan colour.}
3. C_3:={Set of initial points, covered with Cream colour.}

Fig. 10 shows the existence of cyclic attractors in each region. The interesting thing, we have observed here is the disappearance of hidden attractors but the number of cyclic attractors are increasing in proportion to the number of wings. For plotting this figure, we have started selection of initial points from each set and got cyclic attractors inside each wing. For detailed information each attractor, inside each wing, can be seen in Fig. 10 indicated by arrows and bounded in squares.

5 Higher degree of wings with the relation of its basins

In section (4), we have observed the direct proportionality relation between the number of generated wings and cyclic attractors. In other words, one

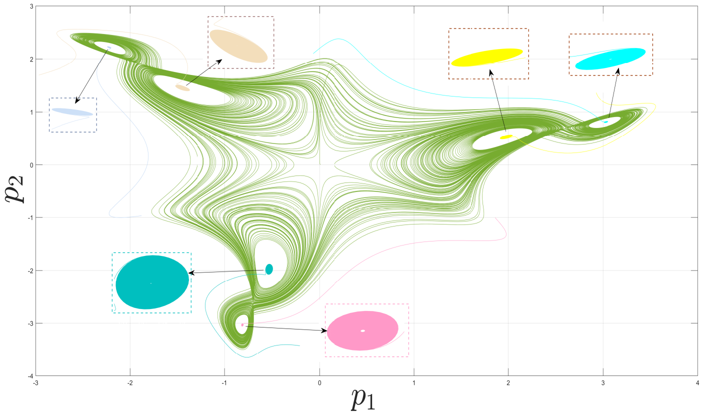

Figure 10. Cyclic attractors in each wing of system (13).

can say that, the more we increase the numbers of wings in chaotic system using Julia procedure, the more cyclic attractors will also be generated. In this section, we will select random dimension to generate wings of system (1) along with its basins, with the aid of procedure discussed in Section (4), to verify the aforementioned relation. Hence, for a generalized $2n$ multi-wings system (1), we have a system has been obtained that can generate the multi-wing chaotic attractors and can be expressed as follows:

$$\begin{aligned}\dot{\mathfrak{u}}_k =&\frac{\bar{\mathrm{R}}}{k\left|\varphi_k^k\right|^{2k-2}}[-k_1\mathrm{R}+k_2\mathrm{S}]\\&-\frac{\bar{\mathrm{S}}}{k\left|\varphi_k^k\right|^{2k-2}}\left[k_3\mathrm{R}-k_4\mathrm{S}+k_5\mathfrak{w}-k_6\mathrm{R}\mathfrak{w}+k_7\right]\\\dot{\mathfrak{v}}_k =&\frac{\bar{\mathrm{S}}}{k\left|\varphi_k^k\right|^{2k-2}}[-k_1\mathrm{R}+k_2\mathrm{S}]\\&+\frac{\bar{\mathrm{R}}}{k\left|\varphi_k^k\right|^{2k-2}}\left[k_3\mathrm{R}-k_4\mathrm{S}+k_5\mathfrak{w}-k_6\mathrm{R}\mathfrak{w}+k_7\right]\\\dot{\mathfrak{w}}_n =&-k_8\mathrm{R}-k_9\mathrm{S}-k_{10}\mathfrak{w}+k_{11}\mathrm{RS}+k_{12}.\end{aligned}\tag{14}$$

System (14) is the generalized equation for the generation of $2k$ wings of our considered model. In the above expression (14), R represents the real and S represents the imaginary parts of polynomial φ_k^k having $k^{th}-$order and are given in Appendix **B**. Here, our concern is with the generation of multiple wings along with cyclic attractors in system (1). Therefore, we select $k = 7$ in Eq. (14) to generate seven similar attractors, fourteen wings and cyclic attractors inside each wing. In Fig. 11, we can see seven

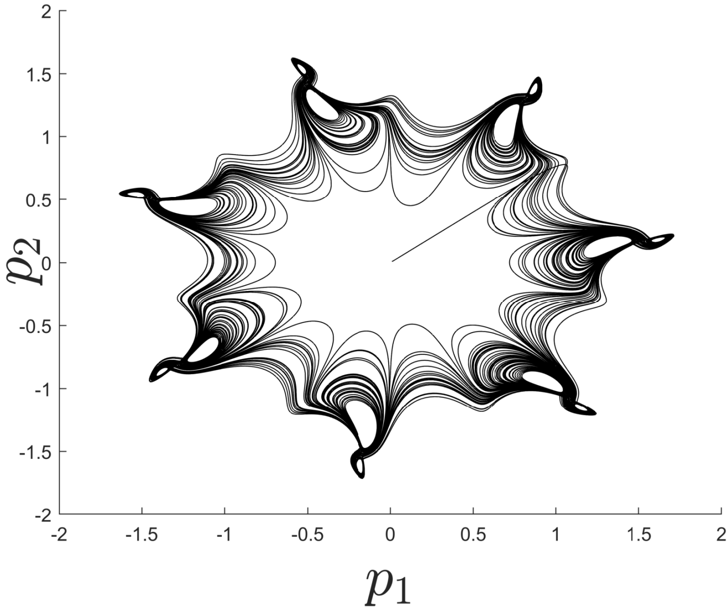

Figure 11. Fractals of chemical system with fourteen wings

similar chaotic attractors and each attractor has double wings. Therefore, fourteen-winged fractals of our considered model are achieved. This is further continued with the achievement of basins of Fig. 11. In Fig. 12, one can see the basin in symmetrical shape and has obtained exactly the same shape of fractals. Similar to the explanation given in previous section (4), one can observe the seven different coloured attracting sets. These sets are responsible for the generation of cyclic attractors inside each wing. Figure 13 is the validation of above explanation about the basins given in Fig. 12, whereas each wing containing cyclic attractors can be seen with the same colour selected as for its basin. This figure shows that

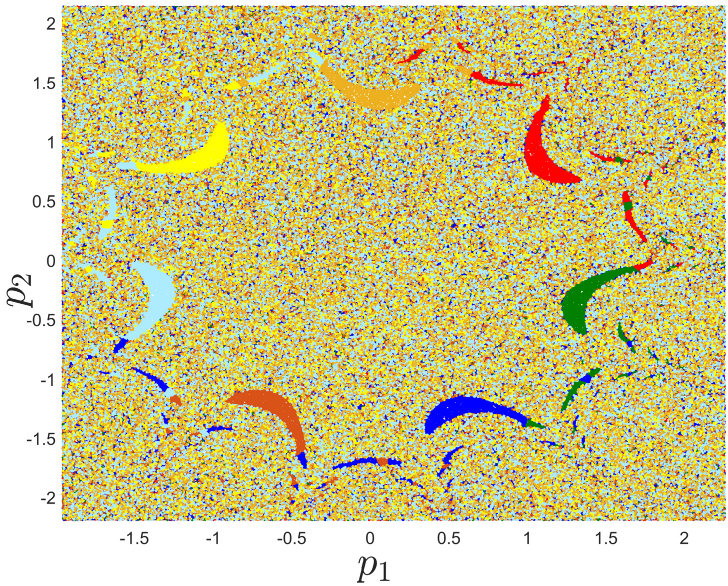

Figure 12. Basins of system (14) with $k = 7$

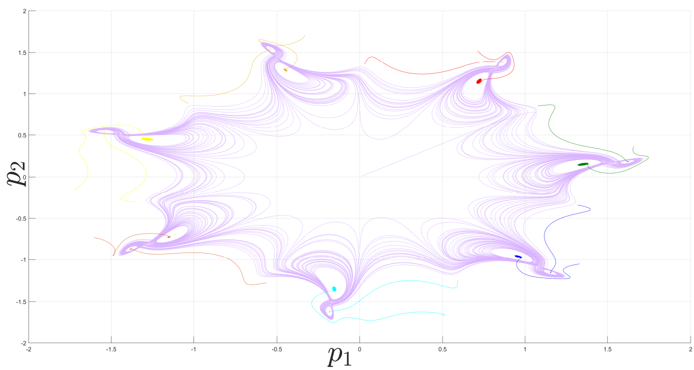

Figure 13. Cyclic attractors in each wing of system (14).

our idea is not limited to two or three wings. The more we generate its wings, the more cyclic attractor can be achieved. Moreover, till now, no one has discussed the concept of basins for fractals. Therefore this idea will open the new door and can solve more riddled questions with the passage of time, related to fractals and chaotic systems.

6 Conclusion

In a chemical system, numerous atomic bonds undergo chemical reactions. However, if the bonds between atoms begin to dissolve and reform into similar tiny structures, fractals are always born. Fractals are always studied in relation to the generation of analogous structures. For this purpose, we have modelled a chemical reaction-based system by introducing modifications in the Lorenz system and adjusting the axis-shifted value. What is the difference between the phase portraits of the original Lorenz system and the one depicted in Figure 1? In section (3), however, we have demonstrated that although the first phase portrait appears similar, the remaining properties are distinct. Using basins, we were able to establish the existence of cyclic and concealed attractors, which is the most significant finding. Using the Julia technique, the dynamics of system (1) were expanded by generating $2k$ chaotic wings. In Figures 5, 8, and 11, the system (1) generates four, six, and fourteen wings, respectively. In addition, the dynamics of additional wings were first achieved by collecting all the initial points in a set known as its basin. For each wing, the basin (shown in Figures 6, 9 and 12) was provided in order to investigate some hidden and deep dynamical aspects. Using these figures, we were able to determine the existence of cyclic attractors in all extra wings through the plotting of Figures 7, 10 and 11.

Appendix A

The Lorenz based chemical reaction is classified into four types, Cooperative catalytic species of constant concentration; **C**, Irreversible source reactions; **S**, Irreversible deletion to an external sink; **E** and Rate limiting; **R**. Moreover, for Rate limiting; **R**, we need to understand the rate determining step. Therefore, the slow and fast reactions can be postulated:

$$\begin{cases} D + \mathfrak{p}_1 + \mathfrak{p}_3 \longrightarrow D^\star + \mathfrak{p}_1 + \mathfrak{p}_3 \ \ (Slow) \\ D^\star + \mathfrak{p}_2 \longrightarrow D + R \ \ (Fast). \end{cases} \tag{15}$$

In accordance with the classifications and Eq. (15) the following reactions can take place for Irreversible source reaction (S): $R \xrightarrow{k_{12}} z, \quad JS = k_{12}$, Cooperative catalytic species of constant concentration; **C**:

	Reactions	Rates
(C_1)	$A + \mathfrak{p}_2 \xrightarrow{k_2} \mathfrak{p}_1 + \mathfrak{p}_2,$	$JC_1 = \mathfrak{p}_2 k_2,$
(C_2)	$B + \mathfrak{p}_1 \xrightarrow{k_3} \mathfrak{p}_2 + \mathfrak{p}_1,$	$JC_2 = \mathfrak{p}_1 k_3,$
(C_3)	$B + \mathfrak{p}_3 \xrightarrow{k_5} \mathfrak{p}_2 + \mathfrak{p}_3,$	$JC_3 = \mathfrak{p}_3 k_5$
(C_4)	$C + \mathfrak{p}_1 + \mathfrak{p}_2 \xrightarrow{k_{11}} \mathfrak{p}_3 + \mathfrak{p}_1 + \mathfrak{p}_2,$	$JC_4 = \mathfrak{p}_1 \mathfrak{p}_2 k_{11},$

(16)

Rate limiting (slow / fast) deletion of variable species; **R**:

	Reactions	Rates
(R_1)	$D + \mathfrak{p}_1 + \mathfrak{p}_3 \xrightarrow[\text{(slow)}]{k_b} D^\star + \mathfrak{p}_1 + \mathfrak{p}_3$ $D^\star + \mathfrak{p}_2 \xrightarrow[\text{(fast)}]{} D + R,$	$JR_1 = \mathfrak{p}_1 \mathfrak{p}_3 k_6$
(R_2)	$D \xrightarrow[\text{(slow)}]{k_7} D^\star, \quad D^\star + \mathfrak{p}_2 \xrightarrow[\text{(fast)}]{} D + R$	$JR_2 = k_7$
(R_3)	$E + \mathfrak{p}_1 \xrightarrow[\text{(slow)}]{k_8} E^\star + \mathfrak{p}_1, \quad E^\star + \mathfrak{p}_3 \xrightarrow[\text{(fast)}]{} E + R$	$JR_3 = \mathfrak{p}_1 k_8,$
(R_4)	$E + \mathfrak{p}_2 \xrightarrow[\text{(slow)}]{k_9} E^\star + \mathfrak{p}_2, \quad E^\star + \mathfrak{p}_3 \xrightarrow[\text{(fast)}]{} E + R$	$JR_4 = \mathfrak{p}_2 k_9$

(17)

and irreversible deletion to an external sink; **E**:

	Reactions	Rates
(E_1)	$\mathfrak{p}_1 \xrightarrow{k_1} R,$	$JE_1 = \mathfrak{p}_1 k_1,$
(E_2)	$\mathfrak{p}_2 \xrightarrow{k_4} R,$	$JE_2 = \mathfrak{p}_2 k_4,$
(E_3)	$\mathfrak{p}_3 \xrightarrow{k_{10}} R,$	$JE_3 = \mathfrak{p}_3 k_{10}.$

(18)

These reactions plays vital role in governing the following dynamical system in terms of constant rates J.

$$\begin{cases} \dot{\mathfrak{p}_1} = -JE_1 + JC_1 \\ \dot{\mathfrak{p}_2} = JC_2 - JE_2 + JC_3 - JR_1 + JR_2 \\ \dot{\mathfrak{p}_3} = -JR_3 - JR_4 - JE_3 + JC_4 + JS, \end{cases} \tag{19}$$

We will get system of chemical reactions (1), by substitute the right side of equations used in Rates column of Eqs. (16-18), into Eq. (19).

Appendix B

In 2016, Guo *et al* [10] derived analytical formulae using Julia process, which Anam *et al* [2] used for the generation of multi-wings in STF model as well. They have defined a mapping from $\phi_k := \mho_n \to \mho = \mho_1$, such that $\phi_k(\pi_k^k, \mathfrak{w})$ for $k \geq 2$, where $\pi_k^k{=}\pi_1{=}\mathfrak{u} + \iota\mathfrak{v}$ is a complex number. The mapping possess a local diffeomorphism with the extra condition that one of the axis will remain unchanged. For ϕ_k, the Jacobian matrix is:

$$\wp\phi_k = \begin{bmatrix} \frac{\partial \mathfrak{u}}{\partial \mathfrak{u}_k} & \frac{\partial \mathfrak{u}}{\partial \mathfrak{v}_k} & 0 \\ \frac{\partial \mathfrak{v}}{\partial \mathfrak{u}_k} & \frac{\partial \mathfrak{v}}{\partial \mathfrak{v}_k} & 0 \\ 0 & 0 & \frac{\partial \mathfrak{w}}{\partial \mathfrak{w}} \end{bmatrix}. \tag{20}$$

The inverse of $\wp\phi_k$ is given as

$$\wp^{-1}\phi_k = \begin{bmatrix} \frac{\bar{\mathrm{R}}}{k|\varphi_k^k|^{2k-2}} & -\frac{\bar{\mathrm{S}}}{k|\varphi_k^k|^{2k-2}} & 0 \\ \frac{\bar{\mathrm{S}}}{k|\varphi_k^k|^{2k-2}} & \frac{\bar{\mathrm{R}}}{k|\varphi_k^k|^{2k-2}} & 0 \\ 0 & 0 & 1 \end{bmatrix}. \tag{21}$$

In Eq. (21), $\bar{\mathrm{R}}$ and and $\bar{\mathrm{S}}$ are the real and imaginary parts of a polynomial φ_k^k having $(k-1)^{th}$ order and is expressed as given in [2, 10]

$$\bar{\mathrm{R}} = \mathrm{Re}\left((\mathfrak{u}_k - i\mathfrak{v}_k)^{k-1}\right)$$
$$= \begin{cases} \mathfrak{u}_k^{k-1} + f_{\bar{\mathrm{R}}}(\mathfrak{u}_k, \mathfrak{v}_k), & \text{if } k \text{is even} \\ \mathfrak{u}_k^{k-1} + g_{\bar{\mathrm{R}}}(\mathfrak{u}_k, \mathfrak{v}_k), & \text{if } k \text{is odd} \end{cases} \tag{22}$$

where

$$f_{\bar{\mathrm{R}}}(\cdot) = \sum_{i=1}^{(k-2)/2} (-1)^i \frac{\Pi_{j=0}^{2i-1}(k-j-1)}{(2i)!} \mathfrak{u}_k^{k-2i-1} \mathfrak{v}_k^{2i},$$
$$g_{\bar{\mathrm{R}}}(\cdot) = \sum_{i=1}^{(k-1)/2} (-1)^i \frac{\Pi_{j=0}^{2i-1}(k-j-1)}{(2i)!} \mathfrak{u}_k^{k-2i-1} \mathfrak{v}_k^{2i}$$

and

$$\bar{\mathrm{S}} = \mathrm{Im}\left((\mathfrak{u}_k - i\mathfrak{v}_k)^{k-1}\right)$$
$$= \begin{cases} f_{\bar{\mathrm{S}}}(\mathfrak{u}_k, \mathfrak{v}_k), \text{ if } k \text{ is even} \\ g_{\bar{\mathrm{S}}}(\mathfrak{u}_k, \mathfrak{v}_k), \text{ if } k \text{ is odd} \end{cases} \tag{23}$$
$$f_{\bar{\mathrm{S}}}(\cdot) = \sum_{i=1}^{k/2} (-1)^i \frac{\Pi_{j=0}^{2i-2}(k-j-1)}{(2i-1)!} \mathfrak{u}_k^{k-2i} \mathfrak{v}_k^{2i-1},$$
$$g_{\bar{\mathrm{S}}}(\cdot) = \sum_{i=1}^{(k-1)/2} (-1)^i \frac{\Pi_{j=0}^{2i-2}(k-j-1)}{(2i-1)!} \mathfrak{u}_k^{k-2i} \mathfrak{v}_k^{2i-1}.$$

Hence, for a generalized $2k$ multi-wings system (1), we have

$$\begin{bmatrix} \dot{\mathfrak{u}}_k \\ \dot{\mathfrak{v}}_k \\ \dot{\mathfrak{w}}_k \end{bmatrix} = \wp_k^{-1} \phi_k \begin{bmatrix} \dot{\mathfrak{u}} \\ \dot{\mathfrak{v}} \\ \dot{\mathfrak{w}} \end{bmatrix} = \begin{bmatrix} \frac{\bar{\mathrm{R}}}{k|\varphi_k^k|^{2k-2}} & -\frac{\bar{\mathrm{S}}}{k|\varphi_k^k|^{2k-2}} & 0 \\ \frac{\bar{\mathrm{S}}}{k|\varphi_k^k|^{2k-2}} & \frac{\bar{\mathrm{R}}}{k|\varphi_k^k|^{2k-2}} & 0 \\ 0 & 0 & 1 \end{bmatrix} \tag{24}$$
$$\times \begin{bmatrix} \Psi_1(\mathfrak{u}_k, \mathfrak{v}_k, \mathfrak{w}) \\ \Psi_2(\mathfrak{u}_k, \mathfrak{v}_k, \mathfrak{w}) \\ \Psi_3(\mathfrak{u}_k, \mathfrak{v}_k, \mathfrak{w}) \end{bmatrix}, \tag{25}$$

whereas the analytical results for Ψ_1, Ψ_2 and Ψ_3 can be achieved by substituting R, S, $\mathfrak{w}$ into Eq. (4) by replacing $\mathfrak{u}$, $\mathfrak{v}$ and $\mathfrak{w}$ respectively

$$\begin{bmatrix} \Psi_1\left(\mathfrak{u}_k, \mathfrak{v}_k, \mathfrak{w}\right) \\ \Psi_2\left(\mathfrak{u}_k, \mathfrak{v}_k, \mathfrak{w}\right) \\ \Psi_3\left(\mathfrak{u}_k, \mathfrak{v}_k, \mathfrak{w}\right) \end{bmatrix} \tag{26}$$

$$= \begin{bmatrix} -k_1\mathrm{R} + k_2\mathrm{S} \\ k_3\mathrm{R} - k_4\mathrm{S} + k_5\mathfrak{w} - k_6\mathrm{R}\mathfrak{w} + k_7 \\ -k_8\mathrm{R} - k_9\mathrm{S} - k_{10}\mathfrak{w} + k_{11}\mathrm{RS} + k_{12}. \end{bmatrix}, \tag{27}$$

where R and S given below show the real and imaginary parts of the polynomial ϕ_k^k

$$\begin{aligned} \mathrm{R} &= \mathrm{Re}\left(\left(\mathfrak{u}_k + \iota\mathfrak{v}_k\right)^k\right) \\ &= \begin{cases} \mathfrak{u}_k^k + f_{\mathrm{R}}\left(\mathfrak{u}_k, \mathfrak{v}_k\right), & \text{if } k \text{ is even} \\ \mathfrak{u}_k^k + g_{\mathrm{R}}\left(\mathfrak{u}_k, \mathfrak{v}_k\right), & \text{if } k \text{ is odd} \end{cases} \end{aligned} \tag{28}$$

$$f_{\mathrm{R}}(\cdot) = \sum_{i=1}^{k/2}(-1)^i\frac{\Pi_{j=0}^{2i-1}(k-j)}{(2i)!}\mathfrak{u}_k^{k-2i}\mathfrak{v}_k^{2i},$$

$$g_{\mathrm{R}}(\cdot) = \sum_{i=1}^{(k-1)/2}(-1)^i\frac{\Pi_{j=0}^{2i-1}(k-j)}{(2i)!}\mathfrak{u}_k^{k-2i}\mathfrak{v}_k^{2i}.$$

and

$$\mathrm{S} = \begin{cases} f_{\mathrm{S}}\left(\mathfrak{u}_k, \mathfrak{v}_k\right), & \text{if } k \text{ is even} \\ g_{\mathrm{S}}\left(\mathfrak{u}_k, \mathfrak{v}_k\right), & \text{if } k \text{ is odd} \end{cases} \tag{29}$$

$$f_{\mathrm{S}}(\cdot) = \sum_{i=1}^{k/2}(-1)^{i+1}\frac{\Pi_{j=0}^{2i-2}(k-j)}{(2i-1)!}\mathfrak{u}_k^{k-2i+1}\mathfrak{v}_k^{2i-1},$$

$$g_{\mathrm{S}}(\cdot) = \sum_{i=1}^{(k+1)/2}(-1)^{i+1}\frac{\Pi_{j=0}^{2i-2}(k-j)}{(2i-1)!}\mathfrak{u}_k^{k-2i+1}\mathfrak{v}_k^{2i-1}.$$

Equations (20−29) are the analytical formulae used in achieving multiple wings, not only in our considered model, but in all chaotic systems as well.

References

[1] A. I. Amen, Integrability analysis of the smallest 3D biochemical reaction model, *MATCH Commun. Math. Comput. Chem.* **90** (2023) 333–356.

[2] A. Azam, M. Aqeel, S. Ahmad, F. Ahmad, Chaotic behavior of modified stretch-twist-fold (STF) flow with fractal property, *Nonlin. Dyn.* **90** (2017) 1–12.

[3] A. Azam, M. Aqeel, D. A. Sunny, Generation of multi-directional mirror symmetric multi-scroll chaotic attractors (MSMCA) in double wing satellite chaotic system, *Chaos Solitons & Fractals* **155** (2022) #111715.

[4] S. Bouali, A. Buscarino, L. Fortuna, M. Frasca, L. V. Gambuzza, Emulating complex business cycles by using an electronic analogue, *Nonlin. Anal. Real World Appl.* **13** (2012) 2459–2465.

[5] G. Chen, T. Ueta, Yet another chaotic attractor, *Int. J. Bifur. Chaos* **9** (1999) 1465–1466.

[6] Q. Din, U. Saeed, Stability, discretization, and bifurcation analysis for a chemical reaction system, *MATCH Commun. Math. Comput. Chem.* **90** (2023) 151–174.

[7] Q. Din, Dynamics and Hopf bifurcation of a chaotic chemical reaction model, *MATCH Commun. Math. Comput. Chem.* **88** (2022) 351–369.

[8] G. Datseris, A. Wagemakers, Effortless estimation of basins of attraction, *Chaos Interdisc. J. Nonlin. Sci.* **32** (2022) #023104.

[9] Y. Guo, J. Yang, B. Liu, Application of chaotic encryption algorithm based on variable parameters in RFID security, *EURASIP J. Wireless Commun. Netw.* **1** (2021) 1–7.

[10] Y. Guo, , G. Qi, Y. Hamam, A multi-wing spherical chaotic system using fractal process, *Nonlin. Dyn.* **85** (2016) 2765–2775.

[11] S. B. He, K. H. Sun, C. X. Zhu, Complexity analyses of multi-wing chaotic systems, *Chinese Phys. B* **22** (2013) #050506.

[12] J. Iqbal, S. Ahmad, M. Marwan, M. Shaukat, Control and numerical analysis for cancer chaotic system, *Archive Appl. Mech.* **90** (2020) 2597–608.

[13] J. Iqbal, S. Ahmad, M. Marwan, A. Rafiq, Control analysis of virotherapy chaotic system, *J. Biol. Dyn.* **31** (2022) 585–595.

[14] K. M. Ibrahim, R. K. Jamal, F. H. Ali, Chaotic behaviour of the Rossler model and its analysis by using bifurcations of limit cycles and chaotic attractors, *Int. J. Phys.* **1003** (2018) #012099.

[15] B. Ibrahim, S. Peter, Persistent subspaces of reaction-based dynamical systems, *MATCH Commun. Math. Comput. Chem.* **90** (2023) 471–494.

[16] A. Jones, N. Strigul, Is spread of COVID-19 a chaotic epidemic? *Chaos Solitons & Fractals* **142** (2021) #110376.

[17] E. C. Jose, D. A. SJ. Talabis, E. R. Mendoza, Absolutely complex balanced kinetic systems, *MATCH Commun. Math. Comput. Chem.* **88** (2022) 397–436.

[18] C. Letellier, L. F. Olsen, S. Mangiarotti, Chaos: From theory to applications for the 80th birthday of Otto E. Rossler, *Chaos Interdisc. J. Nonlin. Sci.* **31** (2021) #060402.

[19] S. Larptwee, W. San-Um, Implementation of Rossler chaotic system through inherent exponential nonlinearity of a diode with two-channel chaotic synchronization applications, *Fourth International Conference on Intelligent Control and Information Processing (ICICIP), IEEE*, 2013, pp. 787–791.

[20] Y. Liu, Exploration and control of bifurcation in a fractional-order delayed glycolytic oscillator model, *MATCH Commun. Math. Comput. Chem.* **90** (2023) 103–149.

[21] L. Lesmoir-Gordon, *The Colours of Infinity: The Beauty and Power of Fractals*, Springer, London, 2004.

[22] W. Li, P. Li, M. Jia, Chaos control and chaos synchronization of a multi-wing chaotic system and its application in multi-frequency weak signal detection, *AIP Adv.* **11** (2021) #095003.

[23] H. Lin, C. Wang, F. Yu, C. Xu, Q. Hong, W. Yao, Y. Sun, An extremely simple multi-wing chaotic system: dynamics analysis, encryption application, and hardware implementation, *IEEE Trans. Indust. El.* **68** (2020) 12708–12719.

[24] S. Mangiarotti, M. Peyre, Y. Zhang, M. Huc, F. Roger, Y. Kerr, Chaos theory applied to the outbreak of COVID-19: an ancillary approach to

decision making in pandemic context, *Epidemiol. Infect.* **148** (2020) #e95.

[25] L. Moysis, E. Petavratzis, C. Volos, H. Nistazakis, I. Stouboulos, A chaotic path planning generator based on logistic map and modulo tactics, *Robot. Autonom. Sys.* **124** (2020) #103377.

[26] M. Marwan, V. Dos Santos, M. Z. Abidin, A. Xiong, Coexisting attractor in a gyrostat chaotic system via basin of attraction and synchronization of two nonidentical mechanical systems, *Mathematics* **10** (2022) #1914.

[27] M. Marwan, M. Z. Abidin, H. Kalsoom, M. Han, Generalized full order observer subject to incremental quadratic constraint (IQC) for a class of fractional order chaotic systems, *Fract. Fractional* **6** (2022) #189.

[28] M. Messias, J. Meneguette, A. de Carvalho Reinol, A. Gokyildirim, A. Akgul, A cubic memristive system with two twin Rossler-type chaotic attractors symmetrical about an invariant plane, *Int. J. Bifur. Chaos* **32** (2022) #2230032.

[29] B. B. Mandelbrot, The fractal geometry of percolation, polymers and almost everything else, in: U. Landman (Ed.), *Statistical Mechanics and Statistical Methods in Theory and Application*, Plenum Press, New York, 1977, pp. 331–342.

[30] R. Miranda, The proto-Lorenz system, *Phys. Lett. A.* **178** (1993) 105–113.

[31] C. Nwachioma, J. H. Perez-Cruz, Analysis of a new chaotic system, electronic realization and use in navigation of differential drive mobile robot, *Chaos Solitons & Fractals* **144** (2021) #110684.

[32] T. Q. Ndlovu, M. L. Shozi, F. P. da Costa, Mathematical investigations of a kinetic model for glycerol hydrogenolysis via heterogeneous catalysis, *MATCH Commun. Math. Comput. Chem.* **88** (2022) 437–460.

[33] H. A. Peker, F. A. Çuha, B. Peker, Kashuri Fundo decomposition method for solving Michaelis-Menten nonlinear biochemical reaction model, *MATCH Commun. Math. Comput. Chem.* **90** (2023) 315–332.

[34] D. Poland, Cooperative catalysis and chemical chaos: a chemical model for the Lorenz equations, *Phys. D Nonlin. Phen.* **65** (1993) 86–99.

[35] J. C. Sprott, Some simple chaotic flows, *Phys. Rev. E.* **50** (1994) R647–R650.

[36] L. Moysis, M. K. Gupta, V. Mishra, M. Marwan, C. Volos, Observer design for rectangular descriptor systems with incremental quadratic constraints and nonlinear outputs – Application to secure communications, *Int. J. Robust Nonlin. Control* **30** (2020) 8139–8158.

[37] M. Sabir, M. Marwan, S. Ahmad, M. Fiaz, F. Khan, Observer and descriptor satisfying incremental quadratic constraint for class of chaotic systems and its applications in a quadrotor chaotic system, *Chaos Solitons & Fractals* **137** (2020) #109874.

[38] I. Szoke, S. Holban, A short introduction in the history of fractals, *9th International Conference on Development and Application Systems*, 2008, pp. 179–181.

[39] S. Sahoo, BK. Roy, Design of multi-wing chaotic systems with higher largest Lyapunov exponent, *Chaos Solitons & Fractals* **157** (2022) #111926.

[40] S. Sahoo, BK. Roy, A new multi-wing chaotic attractor with unusual variation in the number of wings, *Chaos Solitons & Fractals* **164** (2022) #112598.

[41] J. Sprott, A. Xiong, Classifying and quantifying basins of attraction, *Chaos Interdisc. J. Nonlin. Sci.* **25** (2015) #083101.

[42] J. Toth, V. Hars, Orthogonal transforms of the lorenz and rossler equation, *Phys. D* **19** (1986) 135–144.

[43] X. Wang, C. Guanrong, A gallery of Lorenz-like and Chen-like attractors, *Int. J. Bifur. Chaos* **23** (2013) #1330011.

[44] X. Wang, G. Chen, Constructing a chaotic system with any number of equilibria, *Nonlin. Dyn.* **71** (2013) 429–436.

[45] C. Xu, C. Aouiti, Z. Liu, P. Li, L. Yao, Bifurcation caused by delay in a fractional-order coupled oregonator model in chemistry, *MATCH Commun. Math. Comput. Chem.* **88** (2022) 371–396.

[46] A. Xiong, J. C. Sprott, J. Lyu, X. Wang, 3D printing – The basins of tristability in the Lorenz system, *Int. J. Bifur. Chaos* **27** (2017) #1750128.

[47] W. G. Xu, Q. S. Li, A chemical chaotic system derived from Chua's circuit, *J. Chem. Res.* **6** (2002) 295–296.

[48] W. G. Xu, Q. S. Li, Another chemical chaotic attractor for Chua's equation, *Int. J. Bifur. Chaos* **13** (2003) 2715-2718.

[49] W. G. Xu, Q. S. Li, R. Zhu, Stochastic simulation of chemical Chua system, *Int. J. Bifur. Chaos* **14** (2004) 1053-1057.

[50] F. Yu, C. H. Wang, J. W. Yin, A 4-D chaos with fully qualified four-wing type, *Acta Phys. Sin.* **61** (2012) #020506.

[51] M. Yalcin, J. Suykens, J. Vandewalle, S. Ozoguz, Families of scroll grid attractors, *Int. J. Bifur. Chaos Appl. Sci. Eng.* **12** (2002) 23–28.

[52] S. Yu, J. Lu, H. Leung, G. Chen, Design and implementation of n-scroll chaotic attractors from a general jerk circuit, *IEEE Trans. Circuits Sys.* **52** (2005) 1459–1476.

[53] A. Zarei, S. Tavakoli, Design and control of a multi-wing dissipative chaotic system, *Int. J. Dyn. Control* **6** (2018) 140–53.